NIH Public Access
Author Manuscript
Nat Med. Author manuscript; available in PMC 2011 July 18.

Published in final edited form as:
Nat Med. 2007 February ; 13(2): 204–210. doi:10.1038/nm1536.

Angiotensin II type 1 receptor blockade attenuates TGF-β–induced failure of muscle regeneration in multiple myopathic states

Ronald D Cohn[1,2], **Christel van Erp**[1], **Jennifer P Habashi**[2,3], **Arshia A Soleimani**[1], **Erin C Klein**[1], **Matthew T Lisi**[1], **Matthew Gamradt**[1], **Colette M ap Rhys**[1,2], **Tammy M Holm**[1], **Bart L Loeys**[1], **Francesco Ramirez**[4], **Daniel P Judge**[5], **Christopher W Ward**[6], and **Harry C Dietz**[1,2]

[1] McKusick-Nathans Institute of Genetic Medicine, Johns Hopkins University School of Medicine, 733 N Broadway, Baltimore, Maryland 21205, USA

[2] Howard Hughes Medical Institute, Johns Hopkins University School of Medicine, 733 N Broadway, Baltimore, Maryland 21205, USA

[3] Division of Pediatric Cardiology, Department of Pediatrics, Johns Hopkins University School of Medicine, 733 N Broadway, Baltimore, Maryland 21205, USA

[4] Child Health Institute of New Jersey, University of Medicine and Dentistry of New Jersey–Robert Wood Johnson Medical School, 89 French Street, New Brunswick, New Jersey 08901, USA

[5] Division of Cardiology, Department of Medicine, Johns Hopkins University School of Medicine, 720 Rutland Avenue, Baltimore, Maryland 21205, USA

[6] Department of Biochemistry and Molecular Biology, University of Maryland School of Medicine, 655 W. Lombard Street, Baltimore, Maryland 21202, USA

Abstract

Skeletal muscle has the ability to achieve rapid repair in response to injury or disease[1]. Many individuals with Marfan syndrome (MFS), caused by a deficiency of extracellular fibrillin-1, exhibit myopathy and often are unable to increase muscle mass despite physical exercise. Evidence suggests that selected manifestations of MFS reflect excessive signaling by transforming growth factor (TGF)-β (refs. 2,3). TGF-β is a known inhibitor of terminal differentiation of cultured myoblasts; however, the functional contribution of TGF-β signaling to disease pathogenesis in various inherited myopathic states *in vivo* remains unknown[4,5]. Here we show that increased TGF-β activity leads to failed muscle regeneration in fibrillin-1–deficient mice. Systemic antagonism of TGF-β through administration of TGF-β–neutralizing antibody or the

© 2007 Nature Publishing Group

Correspondence should be addressed to H.C.D. (hdietz@jhmi.edu).

Note: Supplementary information is available on the Nature Medicine website.

AUTHOR CONTRIBUTIONS

R.D.C. conducted most of the experiments and wrote the manuscript; C.E. participated in the analysis of the *ex vivo* muscle data; J.P.H. participated in the development and execution of treatment protocols for both fibrillin-1–deficient and *mdx* mice; A.A.S. participated in immunofluorescent analyses; E.C.K., M.G. and T.M.H. maintained the mouse colonies and contributed to tissue harvesting and preparation; M.T.L. and C.M.R. conducted protein expression analyses; B.L.L. contributed to study design and interpretation, F.R. supplied $Fbn1^{mgR/mgR}$ mice and contributed to study design; D.P.J. was extensively involved in analyzing and interpreting all the data; C.W.W. conducted the *ex vivo* analyses of skeletal muscles; H.C.D. supervised all aspects of this study including study design, execution and interpretation, and manuscript preparation.

COMPETING INTERESTS STATEMENT

The authors declare that they have no competing financial interests.

Reprints and permissions information is available online at http://npg.nature.com/reprintsandpermissions

NIH-PA Author Manuscript
NIH-PA Author Manuscript
NIH-PA Author Manuscript

NIH-PA Author Manuscript

NIH-PA Author Manuscript

NIH-PA Author Manuscript

angiotensin II type 1 receptor blocker losartan normalizes muscle architecture, repair and function *in vivo*. Moreover, we show TGF-β–induced failure of muscle regeneration and a similar therapeutic response in a dystrophin-deficient mouse model of Duchenne muscular dystrophy.

MFS is an autosomal-dominant systemic disorder of connective tissue with an estimated prevalence of 1 in 5,000–10,000 individuals[6]. The condition is caused by mutations in *FBN1*, the gene encoding the extracellular matrix protein fibrillin-1 (ref. 6). Clinical manifestations of MFS include bone overgrowth, ocular lens dislocation, emphysema and cardiac complications such as aortic aneurysm. The majority of individuals with MFS lack the ability to increase muscle mass in response to physiologic signals for hypertrophy including growth and exercise. A subset of individuals, prominently those with neonatal onset of severe and rapidly progressive MFS, has profound muscle hypoplasia and hypotonia throughout life. Fibrillin-1 is a structural component of the extracellular matrix microfibril that has been shown to negatively regulate TGF-β activation and signaling[3]. Analyses of fibrillin-1–deficient mice showed that enhanced activation of and signaling by TGF-β contributes directly to failed distal alveolar septation, myxomatous changes of the atrioventricular valves and aortic aneurysm formation[2,3,7].

TGF-β belongs to a family of cytokines that transduce their signal through the SMAD intracellular signaling cascade[8]. In skeletal muscle, *in vitro* evidence suggests that TGF-β impairs myocyte differentiation during myogenesis[1,5,9]. In addition, TGF-β has been thought to be involved in the formation of fibrosis in response to injury, inflammation or disease[9–11]. But a pathogenetic role for TGF-β in other mechanistic aspects of inherited myopathic disorders has not been shown. To investigate a potential role for TGF-β signaling in the development of myopathy in fibrillin-1–deficient mice, we analyzed animals carrying a targeted mutation (C1039G) in exon 25 of the mouse *Fbn1* gene[12]. This mutation is representative of the most common class of mutations causing human MFS; that is, substitutions of cysteine residues in the EGF-like domains of fibrillin-1. Mice homozygous for the C1039G mutation ($Fbn1^{C1039G/C1039G}$) have an emaciated appearance and die between 10 and 14 d of age secondary to aortic dissection[12]. Analysis of 10-d-old wild-type and homozygous mutant litter mates showed a significant ($P < 0.005$) discrepancy in body weight that correlated with architectural abnormalities in all skeletal muscle groups examined (Supplementary Fig. 1 online), including a significant decrease in muscle fiber size (18.5 ± 2 versus 13 ± 1.5 μm; $P < 0.001$) and number (1,504 ± 26 versus 1,380 ± 25 fibers per muscle; $P < 0.001$) and increased amounts of interstitial tissue and fat between muscle fiber bundles in mutant mice. Mice heterozygous for the C1039G mutation ($Fbn1^{C1039G/+}$) recapitulate the dominant nature of human MFS and show phenotypic manifestations in the pulmonary, cardiovascular and skeletal systems[12]. Immunohistochemical staining for fibrillin-1 showed decreased endomysial expression in skeletal muscle from $Fbn1^{C1039G/+}$ mice and humans with MFS (Supplementary Fig. 1). We observed marked variation in fiber size and endomysial fibrosis in both sets of samples (Fig. 1a and Supplementary Fig. 1).

Ligand-activated TGF-β receptors induce phosphorylation of Smad2 and Smad3 (hereafter referred to as pSmad2/3), which form heteromeric complexes with Smad4 that translocate to the nucleus and mediate target gene responses[8]. We observed nuclear accumulation of pSmad2/3 in myofibers of $Fbn1^{C1039G/+}$ mice as compared to wild-type littermates (Fig. 1a and Supplementary Fig. 1), but no nuclear staining in phosphatase-treated tissue sections (data not shown). Further evidence for increased TGF-β signaling derived from analysis of the expression of periostin, a protein known to be induced by TGF-β and expressed in regenerating skeletal muscle[13]. In contrast to wild-type mice, $Fbn1^{C1039G/+}$ mice showed

NIH-PA Author Manuscript

NIH-PA Author Manuscript

NIH-PA Author Manuscript

high expression of periostin in the sarcolemma and endomysial connective tissue of mature and uninjured skeletal muscle (Fig. 1a).

To show a cause-and-effect relationship between excess TGF-β signaling and development of myopathy in *Fbn1*$^{C1039G/+}$ mice, we achieved systemic TGF-β antagonism *in vivo* by intraperitoneal injection of 1 mg/kg or 10 mg/kg neutralizing antibody to TGF-β beginning at 7 weeks of age. Histologic and morphometric assessment showed a decrease in fiber size in *Fbn1*$^{C1039G/+}$ mice (mean fiber size, 1,698 ± 49 μm^2) when compared to wild-type mice (2,622 ± 55 μm^2) that is restored upon treatment with neutralizing antibody to TGF-β (2,443 ± 41 μm^2; $P < 0.005$ and $P < 0.008$ for *Fbn1*$^{C1039G/+}$ mice versus wild-type and *Fbn1*$^{C1039G/+}$ mice versus TGF-β–neutralizing antibody–treated mice, respectively). Moreover, we observed neither nuclear accumulation of pSmad2/3 nor increased periostin staining in *Fbn1*$^{C1039G/+}$ mice treated with neutralizing antibody (Fig. 1a). These data indicate a causal relationship between dysregulated TGF-β signaling and development of skeletal muscle myopathy in a mouse model of MFS.

The presence of multiple atrophic and split fibers in skeletal muscle of fibrillin-1–deficient mice and individuals with MFS is suggestive of abnormal and/or incomplete muscle regeneration (Fig. 1a and Supplementary Fig. 1). To further investigate the potential mechanism by which TGF-β causes the development of skeletal myopathy, we evaluated the response of skeletal muscle to injury induced by snake venom cardiotoxin. Analysis of wild-type skeletal muscle 4 d after cardiotoxin injection showed numerous regenerating muscle fibers (Fig. 1b). In contrast, skeletal muscle of *Fbn1*$^{C1039G/+}$ mice showed delayed regeneration and only scattered newly formed muscle fibers (Fig. 1b).

At 18 d after cardiotoxin injection, wild-type mice showed substantial muscle regeneration, whereas *Fbn1*$^{C1039G/+}$ mice had multiple small fibers with focal areas of fibrosis, indicative of abnormal muscle repair (Fig. 1b). Systemic administration of neutralizing antibody to TGF-β at the time of and 2 weeks after cardiotoxin injection markedly improved the muscle regeneration capacity of the tibialis anterior muscle at 4 and 18 d after injury in *Fbn1*$^{C1039G/+}$ mice (Fig. 1b). Analysis of the cross-sectional myofiber area of tibialis anterior muscle 18 d after cardiotoxin injection showed a reduction in mean fiber size in *Fbn1*$^{C1039G/+}$ mice (1,145 ± 69 μm^2 versus 2,389 ± 51 μm^2 in wild-type mice) that was rescued upon treatment with neutralizing antibody to TGF-β (2,092 ± 47 μm^2; $P < 0.005$ for *Fbn1*$^{C1039G/+}$ mice versus wild-type, and $P < 0.006$ for *Fbn1*$^{C1039G/+}$ mice versus TGF-β–neutralizing antibody–treated *Fbn1*$^{C1039G/+}$ mice; Fig. 1b). Wild-type and both treated and untreated *Fbn1*$^{C1039G/+}$ mice showed nuclear accumulation of pSmad2/3 and high periostin expression 4 d after cardiotoxin injection (data not shown). These findings are consistent with the prior observation of a transient increase in expression of TGF-β1 and periostin within the first 5 d after muscle injury[13]. In contrast, nuclear accumulation of pSmad2/3 and periostin expression persisted in *Fbn1*$^{C1039G/+}$ mice 18 d after injury; this was not observed in wild-type mice and *Fbn1*$^{C1039G/+}$ mice treated with antibody to TGF-β (Fig. 1b). These data suggest that exaggeration or prolongation, or both, of the physiologic spike in TGF-β signaling that attends muscle injury and repair can limit regeneration and culminate in myopathy.

We next investigated whether increased TGF-β signaling alters the performance of satellite cells, a population of cells responsible for muscle regeneration. Analysis of c-met, a marker for quiescent satellite cells, did not show any significant (see Supplementary Fig. 2 online) difference in the number of satellite cells in wild-type and *Fbn1*$^{C1039G/+}$ mice before injury (Supplementary Fig. 2). In contrast, immunohistochemical assessment of M-cadherin, a marker for proliferating satellite cells[14], at 48 h after toxin-induced injury showed fewer positive satellite cells in the tibialis anterior muscle of *Fbn1*$^{C1039G/+}$ mice (15 ± 5 cells per

NIH-PA Author Manuscript

NIH-PA Author Manuscript

NIH-PA Author Manuscript

field) when compared to wild-type mice (42 ± 8 cells per field) or *Fbn1*$^{C1039G/+}$ mice treated with antibody to TGF-β (35 ± 8 cells per field; $P < 0.004$; Supplementary Fig. 2). Myogenin, a myocyte regulatory factor known to be expressed in proliferating and differentiating satellite cells[15], showed a similar decrease in the tibialis anterior muscle of *Fbn1*$^{C1039G/+}$ mice (42 ± 7 positive cells per field) 72 h after cardiotoxin challenge as compared to wild-type mice (63 ± 7 cells per field) or *Fbn1*$^{C1039G/+}$ mice treated with antibody to TGF-β (59 ± 6 cells per field; $P < 0.002$; Supplementary Fig. 2). Together, these findings indicate that augmented TGF-β signaling causes impaired muscle repair by inhibiting satellite cell proliferation and differentiation.

We then determined whether losartan, an angiotensin II type 1 receptor (AT1) antagonist which has been shown to lead to a clinically relevant antagonism of TGF-β in other disease states including chronic renal disease and cardiomyopathy[16,17], has an impact on muscle in fibrillin-1–deficient mice. Losartan is used widely to treat hypertension, has an exceptional tolerance profile in all age groups and can prevent aortic aneurysm in a mouse model of MFS[7]. Long-term treatment (6 months) with losartan fully normalized steady-state muscle architecture in *Fbn1*$^{C1039G/+}$ mice (wild-type mean fiber size, 2,741 ± 69 μm^2; *Fbn1*$^{C1039G/+}$, 1,746 ± 39 μm^2; *Fbn1*$^{C1039G/+}$ plus losartan, 2,527 ± 58 μm^2; $P < 0.008$ for *Fbn1*$^{C1039G/+}$ mice versus wild-type, and $P < 0.009$ for *Fbn1*$^{C1039G/+}$ mice versus losartan-treated *Fbn1*$^{C1039G/+}$ mice, respectively; Fig. 2). Phenotypic rescue correlated with abrogation of TGF-β signaling in mature skeletal muscle and improved muscle function *in vivo* (Fig. 2 and Supplementary Fig. 3 online). Moreover, we found that administration of losartan before cardiotoxin-induced injury markedly improved muscle regeneration in *Fbn1*$^{C1039G/+}$ mice (Fig. 2).

We next questioned whether this mechanism of myopathy was strictly relevant to MFS, or whether we had learned something fundamental about muscle biology that would prove relevant to other muscle disorders. There is descriptive evidence for increased TGF-β activity associated with fibrosis in various genetic and acquired muscle disorders, and it has been shown that administration of decorin (a TGF-β antagonist) can reduce TGF-β activity and collagen content in the diaphragm of dystrophin-deficient *mdx* mice, an animal model for Duchenne muscular dystrophy[11,18]. But a pathogenic contribution of increased TGF-β activity to impaired muscle regeneration in these conditions has not been documented. One key mechanism in the pathogenesis of various degenerative myopathies including some forms of muscular dystrophy is a decline in satellite cell performance and muscle regeneration over time[14,19]. TGF-β emerged as an attractive candidate mediator of these effects. In keeping with this hypothesis, we found nuclear accumulation of pSmad2/3 and sarcolemmal expression of periostin in skeletal muscle of dystrophin-deficient *mdx* mice (Fig. 3a). One complicating factor in interpretation of these data is that myostatin (encoded by *Mstn*), another member of the TGF-β superfamily that suppresses satellite cell activity[20], also signals through the pSmad2/3 cascade[21]. We were able to remove this variable by showing an ongoing increase in nuclear pSmad2/3 and periostin expression in *mdx/Mstn*$^{-/-}$ animals (Fig. 3a). Myostatin antagonism has been shown to ameliorate the muscle phenotype in dystrophin-deficient *mdx* mice[22,23]; however, in contrast to TGF-β, various lines of evidence have shown that myostatin expression is decreased in muscular dystrophy, perhaps as a component of an inadequate physiologic attempt at compensation[24]. Thus, whereas therapeutic strategies aimed at myostatin antagonism may provide some benefit by targeting a parallel pathway, TGF-β antagonism targets a pathway that seems to contribute to the pathogenesis of disease.

We tested the impact of neutralizing antibody to TGF-β and losartan on the regenerative capacity of 9-month-old *mdx* mice. At 4 d after muscle injury, wild-type mice showed numerous myofibers expressing neonatal myosin, a marker for active regeneration (689 ± 19

NIH-PA Author Manuscript

NIH-PA Author Manuscript

NIH-PA Author Manuscript

neonatal myosin-positive fibers per tibialis anterior muscle, Fig. 3b). *Mdx* mice showed significant impairment in this response with fewer neonatal myosin-positive fibers (268 ± 12; Fig. 3b). Treatment with either TGF-β–neutralizing antibody or losartan improved regeneration (556 ± 22 and 513 ± 14 positive fibers, respectively; $P < 0.002$) when compared to untreated *mdx* mice (Fig. 3b). After 18 d, wild-type mice showed complete regeneration, whereas *mdx* mice showed large areas of tissue fibrosis. Again, *mdx* mice treated with neutralizing antibody or losartan showed improved muscle regeneration and diminished fibrosis, as evidenced by reduced vimentin expression (Fig. 3b).

To show that phenotypic benefit from administration of losartan is derived from inhibition of the TGF-β signaling cascade, we performed immunohistologic analysis of target proteins downstream of AT1. Thrombospondin-1 (TSP-1) acts as a potent mediator of angiotensin II–induced TGF-β activation via AT1 (ref. 25). Wild-type mice did not express significant amounts of TSP-1 in skeletal muscle (Fig. 4a). In contrast, we found strong sarcolemmal expression of TSP-1 in the diaphragm and other muscles of *mdx* mice, whereas losartan-treated *mdx* mice showed greatly reduced expression of TSP-1. Moreover, treated *mdx* mice did not show any significant nuclear accumulation of pSmad2 or increased periostin expression (Fig. 4a), indicative of TGF-β antagonism *in vivo*. In theory, losartan might rescue the muscle phenotype in *mdx* mice by restoring the dystrophin-glycoprotein complex through antagonism of AT1-driven ubiquitin-mediated pro-teolysis[26,27]. Expression studies excluded this hypothesis (Supplementary Fig. 4 online).

We next determined whether long-term treatment with losartan has a beneficial impact on steady-state muscle architecture and muscle function in *mdx* mice. Losartan treatment commenced in *mdx* mice at 6 weeks of age, a time of active muscle necrosis associated with cycles of degeneration and regeneration[19]. After 6–9 months of treatment with losartan, analysis of various muscle groups including the diaphragm (the most severely affected skeletal muscle in *mdx* mice[11,19]) and gastrocnemius showed significant attenuation of disease progression in *mdx* mice (Fig. 4b and Supplementary Fig. 4). Evaluation of tissue fibrosis in the diaphragm of treated mice showed a decrease to 18 ± 4% fibrotic area versus 32 ± 5% in untreated *mdx* mice (Fig. 4b; $P < 0.03$). Moreover, assessment of the minimal Feret's diameter variance coefficient, a parameter that provides a sensitive and reliable representation of fiber size heterogeneity and hence dystrophic changes[28], indicated a significant improvement in losartan-treated *mdx* mice when compared to placebo (Fig. 4b; 304.33 ± 12.85 versus 406.17 ± 21.16, respectively; $P < 0.007$).

In contrast to therapeutic strategies aimed at curing muscular dystrophy through replacement of dystrophin, a protein that contributes to the stability of muscle fibers, strategies aimed at induction of muscle regeneration (for example, TGF-β or myostatin antagonism) will not address the pace of muscle destruction. By allowing muscle regeneration to keep pace with destruction, however, one would anticipate an increase in muscle size, the number of muscle fibers and hence muscle performance. In keeping with this hypothesis, young children with Duchenne muscular dystrophy maintain muscle function despite high creatine kinase levels in serum (indicative of a high rate of muscle fiber destruction). Functional decline correlates with loss of regenerative capacity and progressive fibrotic changes. As predicted by this scenario, there was no significant decrease in creatine kinase levels in losartan-treated *mdx* mice, when compared to untreated animals (data not shown).

To assess whether there was a functional benefit of losartan treatment in *mdx* mice, we performed grip-strength testing *in vivo*. After 6 months of treatment, *mdx* mice showed increased fore-limb (data not shown) and hindlimb grip strength when compared to untreated *mdx* mice (Supplementary Fig. 4). In addition, losartan-treated mice showed

NIH-PA Author Manuscript

NIH-PA Author Manuscript

NIH-PA Author Manuscript

significantly (see Supplementary Fig. 3) less muscle fatigue in response to repetitive challenge.

We next analyzed physiological properties of explanted extensor digitorum longus (EDL) muscles derived from 1-year-old wild-type, *mdx* and losartan-treated *mdx* mice (9 months of treatment). Treated *mdx* mice showed an increase in body and EDL wet muscle weight and cross-sectional area (Supplementary Table 1 online). When compared to untreated *mdx* mice, the losartan-induced increase in EDL muscle mass correlated with a significant increase in the number of fibers per muscle, a significant decrease in the minimal Feret's diameter variance coefficient and no demonstrable increase in single fiber area (Supplementary Table 1). The explanted EDL from losartan-treated mice generated significantly more absolute force over a wide range of stimulation intensities (60–150 Hz) when compared to untreated *mdx* mice; indeed, the performance was statistically indistinguishable from wild-type mice (Fig. 4c and Supplementary Table 1). At submaximal stimulation frequencies (60 and 80 Hz), the increase in force generation was proportional to the increase in muscle area, probably indicative of increased fiber number. At maximal stimulation frequency (100 and 150 Hz), however, the force generation indexed to cross-sectional area was significantly greater in losartan-treated *mdx* mice when compared to placebo (Fig. 4c), plausibly reflecting both an increase in fiber number and a decrease in fibrosis.

Excessive TGF-β signaling has been shown to drive pathology in multiple tissues in MFS, albeit by different mechanisms. In skeletal muscle, we showed that increased TGF-β activity impedes the physiologic response of satellite cells to regenerate muscle in multiple genetically defined forms of myopathy, a process essential for the preservation of muscle architecture and performance. Although losartan does not 'cure' the disease by restoring dystrophin expression or eliminating muscle membrane fragility, or both, the observations of an enduring ability of muscle regeneration to keep pace with destruction and improved muscle function in the *mdx* mouse model support speculation that losartan will improve the quality of life and delay death for individuals with Duchenne muscular dystrophy. The benefits of losartan treatment may extend to other states associated with accelerated muscle injury and/or an inadequate response of satellite cells including other inherited or acquired myopathies, catastrophic muscle injury and aging.

METHODS

Mice

All mouse protocols were approved by the Animal Care and Use Committee of Johns Hopkins University School of Medicine. Creation of the mouse line harboring the *Fbn1* mutation C1039G has been previously described[12]. We performed all analyses in male mice after backcrossing (more than nine times) this mutation into the C57BL/6J background, allowing valid comparisons between litters. Mice were killed with an inhalation overdose of halothane (Sigma-Aldrich). For muscle regeneration experiments in $Fbn1^{C1039G/+}$ mice, we injected 100 μl cardiotoxin (10 μM *Naja nigricollis*; Calbiochem)[13,19] into the tibialis anterior muscle of wild-type and $Fbn1^{C1039G/+}$ mice either treated with TGF-β–neutralizing antibody ($n = 6$ in each group) at 4 months of age or left untreated. Subsequently, we analyzed mice at 4 and 18 d after injury. For regeneration experiments in *mdx* mice, we injected 150 μl cardiotoxin into the tibialis anterior muscle of wild-type and *mdx* mice, either treated with TGF-β–neutralizing antibody ($n = 6$ each group) at 9 months of age or left untreated and analyzed skeletal muscle at 4 and 18 d after injection. The mouse model of MFS used for functional studies is homozygous for a hypomorphic *Fbn1* allele ($Fbn1^{mgR/mgR}$)[29] that expresses normal fibrillin-1 at a level that approximates 15% of normal. This mouse line recapitulates the aortic, lung and valve pathology seen in

NIH-PA Author Manuscript

NIH-PA Author Manuscript

NIH-PA Author Manuscript

Fbn1$^{C1039G/+}$ mice albeit at an accelerated rate[12,29]. The same is true for skeletal muscle (data not shown), enhancing the potential to observe and rescue a functional deficit.

TGF-β–neutralizing antibody treatment

Wild-type and *Fbn1*$^{C1039G/+}$ mice received intraperitoneal injections of TGF-β–neutralizing antibody (R&D Systems), once every 2 weeks starting at 7 weeks of age. Both TGF-β isoforms 1 and 2 are neutralized *in vivo* and *in vitro* by this antibody[2,3]. We diluted the antibody in PBS (pH 7.4) and administered it at a dose of 1 mg/kg or 10 mg/kg body weight. We administered rabbit IgG (10 mg/kg; Zymed Laboratories Inc.) in a similar fashion as a negative control. Mice were killed after 2 months of treatment, and we used a minimum of six mice per genotype for histologic and morphometric analyses. There was no effect on the morphology of wild-type skeletal muscle at either dose (data not shown).

Losartan treatment

Wild-type and *Fbn1*$^{C1039G/+}$ mice started on treatment at 7 weeks of age with oral losartan (0.6 g/L[7] in drinking water; $n = 5$) or placebo ($n = 10$). Mice were continued on oral therapy for 6 months and then killed. For muscle regeneration experiments, we placed 4-month-old fibrillin-deficient and 9–10-month-old *mdx* mice on losartan for 14 d before we injected cardiotoxin. Mice ($n = 4$) continued on losartan for the entire period after cardiotoxin-induced injury. To monitor long-term benefits of losartan treatment, we started male and female *mdx* mice ($n = 6$ each group) on losartan at the age of 6 weeks. Age-matched wild-type and *mdx* mice (placebo-treated) served as a control group. Losartan treatment did not influence the body weight and/or steady state muscle architecture of wild-type mice (data not shown). For *in vivo* and *in vitro* muscle performance, see Supplementary Methods online.

Histology and skeletal muscle morphometry

For morphometric analyses, we flash-froze skeletal muscle in cooled isopentane and mounted it in Tragacanth (Sigma Aldric). Subsequently, we stained 10 μm sections with hematoxylin and eosin. We counted muscle fibers in a defined area (9 mm^2) of the tibialis anterior muscle of 10-d-old wild-type ($n = 3$) and *Fbn1*$^{C1039G/C1039G}$ mice ($n = 6$), and determined fiber diameter by measuring the shortest fiber axis within cross-sections of the tibialis anterior muscle, counting a total of 850–1,500 fibers. The cross-sectional area of undamaged and regenerating myofibers of the tibialis anterior muscle from wild-type and *Fbn1*$^{C1039G/+}$ mice was expressed as a distribution of the percentage of the total number of myofibers analyzed (850–1,500)[30]. We took sections of skeletal muscle within the same anatomical region of the mid-belly of the tibialis anterior muscle. We scored the number of c-met–, M-cadherin– and myogenin-positive cells in 50 fields of the tibialis anterior muscle mid-belly area using the ×40 objective. We scored at least six mice per genotype, and all analyses were performed by investigators blinded to genotype and treatment group. All images were taken using an Eclipse E400 microscope (Nikon Inc.), and cross-sectional area measurements were determined using IPLAB software (Scanalytics).

We determined the minimal Feret's diameter in diaphragm and EDL muscles of wild-type, *mdx* and losartan-reated *mdx* mice ($n = 4$–6 per group) using the Nikon NS elements 2.0 software. We analyzed a minimum of 2,000 fibers for the diaphragm, and we counted all muscle fibers of the EDL. The minimal Feret's diameter is defined as the minimum distance between parallel tangents at opposing borders of the muscle fiber and has been found to be very insensitive to deviations from the optimal cross-sectioning profile[28]. Furthermore, determination of the variance coefficient of the minimal Feret's diameter (s.d. of the muscle fiber/mean muscle fiber size × 1,000) is a reliable method for distinguishing dystrophic from nondystrophic muscle[28].

NIH-PA Author Manuscript

NIH-PA Author Manuscript

NIH-PA Author Manuscript

We quantified neonatal myosin-positive fibers after cardiotoxin challenge by counting 900–1,240 fibers per toxin-challenged muscle ($n = 4$). For quantification of fibrotic tissue formation in toxin-challenged mice ($n = 4$), we performed immunofluorescent staining for vimentin. We analyzed five sections throughout the entire tibialis anterior muscle at low magnification and calculated vimentin-positive areas as a percentage of the total muscle area using the US National Institutes of Health Scion image software, public domain. Similarly, we used van Gieson– and vimentin-stained sections to delineate the percentage of fibrotic versus total muscle area in diaphragm and gastrocnemius of long-term losartan-treated, placebo-treated *mdx* and wild-type mice ($n = 6$ each group) using the Nikon NS elements 2.0 software. For evaluation of percent centrally located nuclei, we visually assessed all fibers of the EDL muscles. We performed analyses of skeletal muscle from human MFS ($n = 4$) on flash-frozen samples.

Immunofluorescence

We performed immunofluorescence studies as previously described[19]. We performed staining of satellite cells on frozen sections fixed in 4% paraformaldehyde, then washed them in PBS containing 0.3% Triton X for 15 min and subsequently blocked them with 5% BSA. We used the following antibodies in this study: goat polyclonal antibody to pSmad2/3, rabbit polyclonal antibody to c-met and rabbit polyclonal antibody to myogenin (all from Santa Cruz Biotechnology Inc.); rabbit polyclonal antibody to pSmad2 (Cell Signal); rat polyclonal antibody to laminin γ1, rabbit polyclonal antibody to dystrophin, rabbit polyclonal antibody to thrombo-spondin-1 and rabbit polyclonal antibody to periostin (all from Abcam); rabbit polyclonal antibody to fibrillin-1 (pAb 9543)[12]; goat polyclonal antibody to vimentin (Sigma); mouse monoclonal antibody to beta-sarcoglycanl mouse and monoclonal antibody to developmental myosin (Novocastra). Antibody to α-dystroglycan IIH6 was supplied by K. Campbell (University of Iowa). We applied secondary Alexa fluor–conjugated donkey antibody to rabbit, rat and mouse IgM and IgG1 and antibody to goat conjugated antibodies (Molecular Probes) for 1 h at room temperature (25 °C). We stained nuclei with DAPI for 5 min and mounted inverted coverslips onto glass slides using Cytoseal (Vector Laboratories).

Statistical analysis

All values are expressed as mean ± s.e.m. To determine significance between two groups, we made comparisons using the unpaired Student *t*-tests. We performed analyses of multiple groups using one-way ANOVA with $P < 0.05$ considered statistically significant.

Supplementary Material

Refer to Web version on PubMed Central for supplementary material.

Acknowledgments

We would like to thank K. Wagner and S.-J. Lee for providing muscle samples of *mdx Mstn*$^{-/-}$ mice. We would like to thank P. Sponseller for providing human muscle samples. H.C. Dietz is an Investigator of the Howard Hughes Medical Institute and is also supported by the US National Institutes of Health, the Smilow Center for Marfan Syndrome Research, the Dana and Albert "Cubby Broccoli Center for Aortic Diseases and the National Marfan Foundation.

References

1. Charge SB, Rudnicki MA. Cellular and molecular regulation of muscle regeneration. Physiol Rev. 2004; 84:209–238. [PubMed: 14715915]

NIH-PA Author Manuscript

NIH-PA Author Manuscript

NIH-PA Author Manuscript

2. Ng CM, et al. TGF-beta-dependent pathogenesis of mitral valve prolapse in a mouse model of Marfan syndrome. J Clin Invest. 2004; 114:1586–1592. [PubMed: 15546004]
3. Neptune ER, et al. Dysregulation of TGF-beta activation contributes to pathogenesis in Marfan syndrome. Nat Genet. 2003; 33:407–411. [PubMed: 12598898]
4. Allen RE, Boxhorn LK. Inhibition of skeletal muscle satellite cell differentiation by transforming growth factor-beta. J Cell Physiol. 1987; 133:567–572. [PubMed: 3480289]
5. Olson EN, Sternberg E, Hu JS, Spizz G, Wilcox C. Regulation of myogenic differentiation by type beta transforming growth factor. J Cell Biol. 1986; 103:1799–1805. [PubMed: 3465734]
6. Dietz HC, et al. Marfan syndrome caused by a recurrent de novo missense mutation in the fibrillin gene. Nature. 1991; 352:337–339. [PubMed: 1852208]
7. Habashi JP, et al. Losartan, an AT1 antagonist, prevents aortic aneurysm in a mouse model of Marfan syndrome. Science. 2006; 312:117–121. [PubMed: 16601194]
8. Heldin CH, Miyazono K, ten Dijke P. TGF-beta signalling from cell membrane to nucleus through SMAD proteins. Nature. 1997; 390:465–471. [PubMed: 9393997]
9. Li Y, et al. Transforming growth factor-beta1 induces the differentiation of myogenic cells into fibrotic cells in injured skeletal muscle: a key event in muscle fibrogenesis. Am J Pathol. 2004; 164:1007–1019. [PubMed: 14982854]
10. Sato K, et al. Improvement of muscle healing through enhancement of muscle regeneration and prevention of fibrosis. Muscle Nerve. 2003; 28:365–372. [PubMed: 12929198]
11. Gosselin LE, et al. Localization and early time course of TGF-beta 1 mRNA expression in dystrophic muscle. Muscle Nerve. 2004; 30:645–653. [PubMed: 15389721]
12. Judge DP, et al. Evidence for a critical contribution of haploinsufficiency in the complex pathogenesis of Marfan syndrome. J Clin Invest. 2004; 114:172–181. [PubMed: 15254584]
13. Goetsch SC, Hawke TJ, Gallardo TD, Richardson JA, Garry DJ. Transcriptional profiling and regulation of the extracellular matrix during muscle regeneration. Physiol Genomics. 2003; 14:261–271. [PubMed: 12799472]
14. Reimann J, Irintchev A, Wernig A. Regenerative capacity and the number of satellite cells in soleus muscles of normal and mdx mice. Neuromuscul Disord. 2000; 10:276–282. [PubMed: 10838255]
15. Jin Y, et al. Expression of MyoD and myogenin in dystrophic mice, mdx and dy, during regeneration. Acta Neuropathol (Berl). 2000; 99:619–627. [PubMed: 10867795]
16. Lavoie P, et al. Neutralization of transforming growth factor-beta attenuates hypertension and prevents renal injury in uremic rats. J Hypertens. 2005; 23:1895–1903. [PubMed: 16148614]
17. Lim DS, et al. Angiotensin II blockade reverses myocardial fibrosis in a transgenic mouse model of human hypertrophic cardiomyopathy. Circulation. 2001; 103:789–791. [PubMed: 11171784]
18. Yamazaki M, et al. Expression of transforming growth factor-beta 1 and its relation to endomysial fibrosis in progressive muscular dystrophy. Am J Pathol. 1994; 144:221–226. [PubMed: 8311110]
19. Cohn RD, et al. Disruption of DAG1 in differentiated skeletal muscle reveals a role for dystroglycan in muscle regeneration. Cell. 2002; 110:639–648. [PubMed: 12230980]
20. Lee SJ. Regulation of muscle mass by myostatin. Annu Rev Cell Dev Biol. 2004; 20:61–86. [PubMed: 15473835]
21. Zhu X, Topouzis S, Liang LF, Stotish RL. Myostatin signaling through Smad2, Smad3 and Smad4 is regulated by the inhibitory Smad7 by a negative feedback mechanism. Cytokine. 2004; 26:262–272. [PubMed: 15183844]
22. Wagner KR, McPherron AC, Winik N, Lee SJ. Loss of myostatin attenuates severity of muscular dystrophy in mdx mice. Ann Neurol. 2002; 52:832–836. [PubMed: 12447939]
23. Bogdanovich S, et al. Functional improvement of dystrophic muscle by myostatin blockade. Nature. 2002; 420:418–421. [PubMed: 12459784]
24. Tkatchenko AV, et al. Identification of altered gene expression in skeletal muscles from Duchenne muscular dystrophy patients. Neuromuscul Disord. 2001; 11:269–277. [PubMed: 11297942]
25. Zhou Y, Poczatek MH, Berecek KH, Murphy-Ullrich JE. Thrombospondin 1 mediates angiotensin II induction of TGF-beta activation by cardiac and renal cells under both high and low glucose conditions. Biochem Biophys Res Commun. 2006; 339:633–641. [PubMed: 16310163]

NIH-PA Author Manuscript

NIH-PA Author Manuscript

NIH-PA Author Manuscript

26. Delafontaine P, Akao M. Angiotensin II as candidate of cardiac cachexia. Curr Opin Clin Nutr Metab Care. 2006; 9:220–224. [PubMed: 16607120]

27. Assereto S, et al. Pharmacological rescue of the dystrophin-glycoprotein complex in Duchenne and Becker skeletal muscle explants by proteasome inhibitor treatment. Am J Physiol Cell Physiol. 2006; 290:C577–C582. [PubMed: 16192300]

28. Briguet A, Courdier-Fruh I, Foster M, Meier T, Magyar JP. Histological parameters for the quantitative assessment of muscular dystrophy in the mdx-mouse. Neuromuscul Disord. 2004; 14:675–682. [PubMed: 15351425]

29. Pereira L, et al. Targetting of the gene encoding fibrillin-1 recapitulates the vascular aspect of Marfan syndrome. Nat Genet. 1997; 17:218–222. [PubMed: 9326947]

30. Horsley V, Jansen KM, Mills ST, Pavlath GK. IL-4 acts as a myoblast recruitment factor during mammalian muscle growth. Cell. 2003; 113:483–494. [PubMed: 12757709]

NIH-PA Author Manuscript

NIH-PA Author Manuscript

NIH-PA Author Manuscript

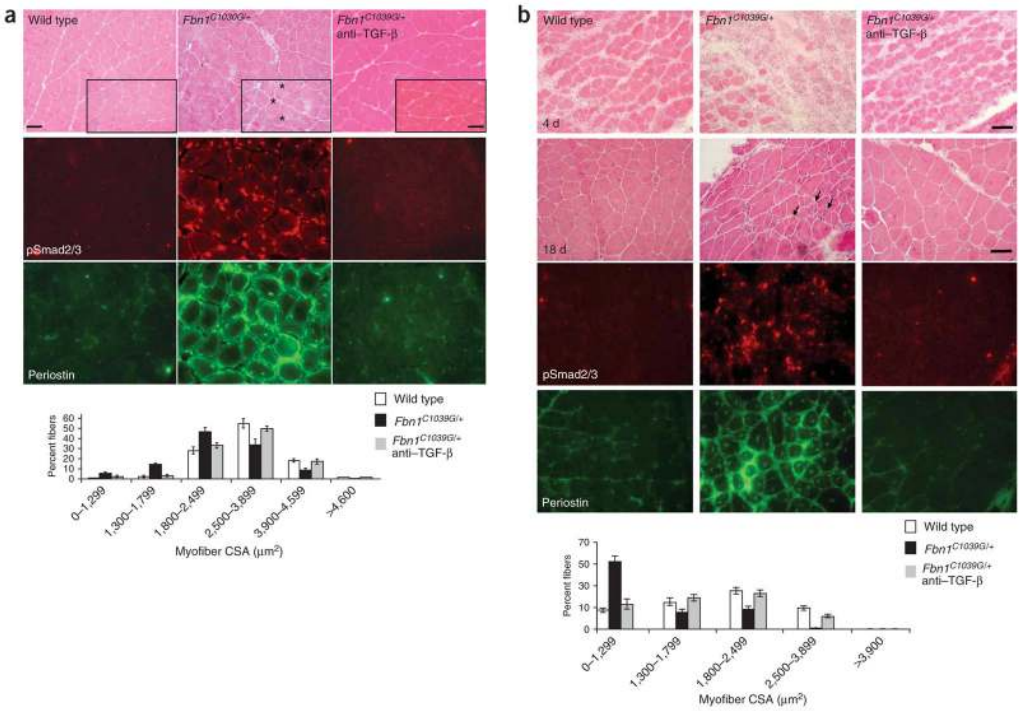

Figure 1.

Evaluation of steady-state and regenerating skeletal muscles in fibrillin-1 deficient mice. (**a**) Hematoxylin and eosin staining of quadriceps muscle (upper panels) shows marked variation of fiber size in *Fbn1*$^{C1039G/+}$ mice. Note several small and split fibers (asterisks), fibers with central nucleation and endomysial thickening. TGF-β antagonism *in vivo* reverses myopathic architecture in *Fbn1*$^{C1039G/+}$ mice. Increased TGF-β signaling, as evidenced by nuclear accumulation of pSmad2/3 (middle panels) and periostin expression (lower panels) in *Fbn1*$^{C1039G/+}$ mice, when compared to wild-type mice or *Fbn1*$^{C1039G/+}$ mice treated with TGF-β–neutralizing antibody. Analysis of the cross-sectional area (myofiber CSA in μm^2) of tibialis anterior muscle fibers shows a decrease in fiber size in *Fbn1*$^{C1039G/+}$ mice when compared to wild-type mice or *Fbn1*$^{C1039G/+}$ mice treated with TGF-β–neutralizing antibody (graph). Scale bars, 70 μm (low magnification) and 50 μm (high magnification, inset boxes). (**b**) Impaired muscle regeneration in *Fbn1*$^{C1039G/+}$ mice. Few newly-formed muscle fibers and disorganized muscle architecture with numerous small fibers (arrows) 4 and 18 days after cardiotoxin-induced muscle injury, respectively, in *Fbn1*$^{C1039G/+}$ mice, when compared to wild-type mice or *Fbn1*$^{C1039G/+}$ mice treated with TGF-β–neutralizing antibody (top panels). Increased TGF-β signaling, as evidenced by increased nuclear accumulation of pSmad2/3 and periostin expression in *Fbn1*$^{C1039G/+}$ mice, when compared to wild-type mice or mice treated with TGF-β–neutralizing antibody (bottom panels). Morphometric analyses of tibialis anterior muscle 18 d after cardiotoxin injection shows reduced myofiber CSA (in μm^2) in *Fbn1*$^{C1039G/+}$ mice, when compared to wild-type mice or *Fbn1*$^{C1039G/+}$ mice treated with TGF-β–neutralizing antibody (graph). Scale bars, 40 μm.

NIH-PA Author Manuscript

NIH-PA Author Manuscript

NIH-PA Author Manuscript

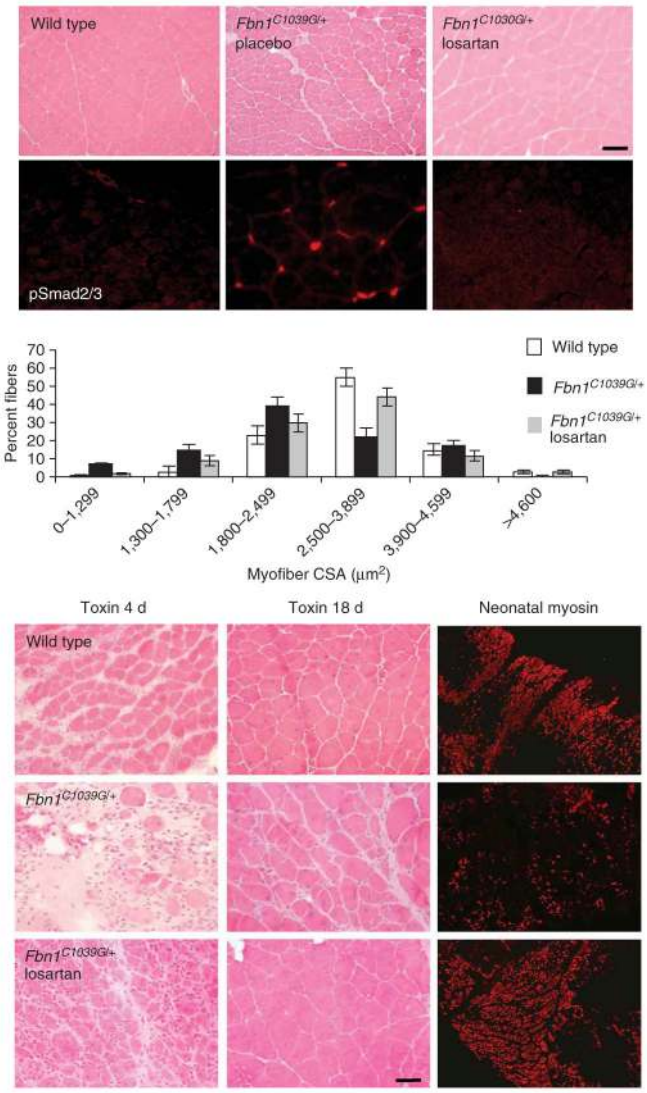

Figure 2.

Losartan antagonizes TGFβ and restores muscle architecture and regeneration in *Fbn1*$^{C1039G/+}$ mice. Placebo-treated *Fbn1*$^{C1039G/+}$ mice show altered quadriceps steady-state muscle architecture with smaller fiber size and nuclear accumulation of pSmad2/3, when compared to wild-type or losartan-treated *Fbn1*$^{C1039G/+}$ mice (top panels). Scale bar, 70 μm. Morphometric analyses showed reduced muscle fiber CSA (in μm^2) in *Fbn1*$^{C1039G/+}$ mice, when compared to wild-type or losartan-treated *Fbn1*$^{C1039G/+}$ mice (graph). Few newly-formed muscle fibers with low neonatal myosin expression and disorganized muscle architecture 4 and 18 days after cardiotoxin-induced muscle injury, respectively, in *Fbn1*$^{C1039G/+}$ mice, when compared to wild-type or losartan-treated *Fbn1*$^{C1039G/+}$ mice (bottom panels). Scale bar, 40 μm.

NIH-PA Author Manuscript

NIH-PA Author Manuscript

NIH-PA Author Manuscript

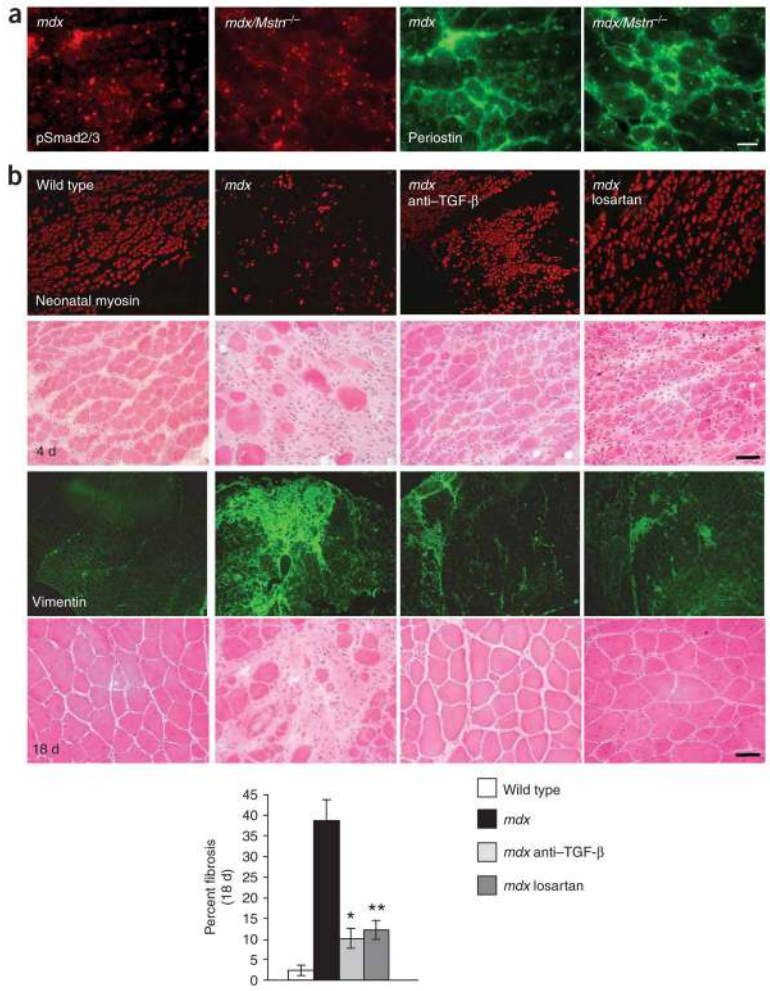

Figure 3.

Increased TGF-β signaling contributes to impaired muscle regeneration in *mdx* mice. (**a**) Increased nuclear accumulation of pSmad2/3 and sarcolemmal and extracellular matrix expression of periostin in dystrophin-deficient *mdx* mice (left panels) and mice deficient in both dystrophin and myostatin (*mdx/Mstn*$^{-/-}$; right panels). Scale bar, 60 μm. (**b**) Reduced new fiber formation and neonatal myosin expression 4 days after cardiotoxin-induced injury in *mdx* mice, when compared to wild-type mice or *mdx* mice treated with TGF-β–neutralizing antibody or losartan (top panels). Extensive fibrosis (as evidenced by vimentin staining) and disorganized muscle architecture 18 days after muscle injury in mdx mice, when compared to wild-type mice or *mdx* mice treated with TGF-β–neutralizing antibody or losartan (bottom panels). The graph shows the percentage of fibrotic area as compared to the total area of muscle tissue 18 days after cardiotoxin injection. *$P < 0.007$ for *mdx* mice treated with TGF-β–neutralizing antibody versus untreated *mdx* mice; **$P < 0.005$ for losartan-treated versus untreated *mdx* mice. Scale bars, 40 μm.

NIH-PA Author Manuscript

NIH-PA Author Manuscript

NIH-PA Author Manuscript

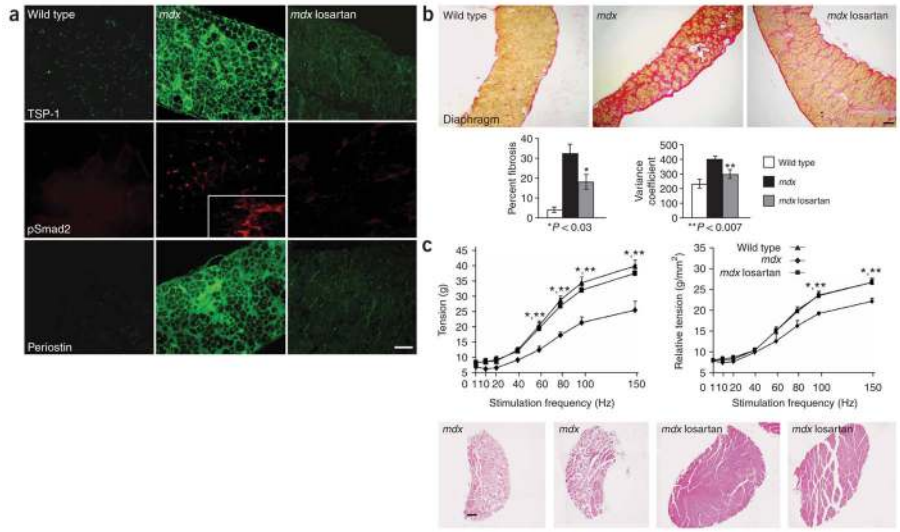

Figure 4.

Losartan decreases angiotensin II-mediated TGF-β signaling and improves muscle function in *mdx* mice. (**a**) Immunofluorescence analysis of target proteins downstream of the AT1. The diaphragm of *mdx* mice shows increased expression of thrombospondin-1 (TSP-1), a potent activator of TGF-β, and increased nuclear accumulation of pSmad2 and sarcolemmal and matrix expression of peripostin, when compared to wild-type or losartan-treated *mdx* mice. The inset box shows nuclear accumulation of pSmad2 in a connective tissue-rich region of diseased muscle. Scale bar, 100 μm. (**b**) Long-term losartan treatment attenuated myopathic disease progression in 9 month-old *mdx* mice. Representative sections of van Gieson–stained diaphragm from wild-type, *mdx* and losartan-treated *mdx* mice. Losartan-treated mice showed significantly (*P* 0.03) less fibrosis (red) than untreated *mdx* mice. Scale bar, 150 μm. The graphs show quantification of fibrotic area, expressed as percentage of total muscle area (left), and minimal Feret's diameter variance coefficient (right). (**c**) *In vitro* force-frequency relationship of explanted EDL muscle. Isometric tension (g) versus stimulation frequency (1–150 Hz) was reduced in *mdx* mice at frequencies equal to or greater than 60 Hz, but was fully restored in losartan-treated *mdx* mice, as compared to wild-type animals (*wild-type versus *mdx* mice, **losartan-treated versus untreated *mdx* mice, $P < 0.05$; left graph). When force was normalized to muscle cross-sectional area (relative tension), losartan-treated *mdx* and wild-type mice were indistinguishable, whereas untreated *mdx* mice showed a significant decrease at frequencies of 100 and 150 Hz, when compared to either wild-type or losartan-treated *mdx* mice, (*wild-type versus *mdx* mice, **losartan-treated versus untreated *mdx* mice, $P < 0.05$; right graph). Representative low-power whole-muscle montages of EDL muscles from two untreated *mdx* mice (left) showed an overall decrease in muscle size and fiber content and an increase in fibrosis, as compared to two losartan-treated *mdx* mice (right). Wild-type mice, $n = 4$; untreated *mdx* mice, $n = 3$; losartan-treated *mdx* mice, $n = 4$. Scale bar, 150 μm.